

Common Control Channel Allocation in Cognitive Radio Networks through UWB Communication

A. Masri[†], C.-F. Chiasserini[†], C. Casetti[†], A. Perotti^{*}

[†] Politecnico di Torino, Italy, Email: firstname.lastname@polito.it

^{*} CSP-ICT Innovation, Italy, Email: alberto.perotti@csp.it

Abstract—The implementation of a common control channel is one of the most challenging issues in cognitive radio networks, since a fully reliable control channel cannot be created without reserving bandwidth specifically for this purpose. In this paper, we investigate a promising solution that exploits the Ultra Wide Band (UWB) technology to let cognitive radio nodes discover each other and exchange control information for establishing a communication link. The contribution of this paper is threefold: (i) we define the communication protocol needed to let cognitive radio nodes discover each other and exchange control information for link set up, (ii) we overcome the gap in coverage, which typically exists between UWB and long-medium range technologies, by using multi-hop communication, (iii) we evaluate the performance of our approach by adopting an accurate channel model and show its benefits with respect to an in-band signalling solution.

I. INTRODUCTION

Recently, the possibility to open licensed frequency bands to unlicensed operations has been considered, with the aim to improve the utilization of these portions of the spectrum. This new regulatory model requires the development of cognitive radio (CR) devices that are able to detect spectrum opportunities in licensed bands and map them into logical channels, which can be used for communication while the selected frequencies remain available. CR nodes are typically called secondary users, to differentiate them from licensed owners of spectrum bands, i.e., primary users.

In this work, we consider a distributed system architecture where no central controller is required. In such a scenario, one of the major issues is the implementation of a common control channel (CCC) [1], over which CR nodes can (i) discover each other and establish a first contact, (ii) coordinate their access to the spectrum, and (iii) identify common spectrum opportunities to set up data communication on those frequencies. As observed in [2], independently of the adopted medium access control (MAC) scheme, the operation in (i) is at the basis of any communication: given two CR nodes, which may sense a different set of channels as available, they need to *meet* on a channel that is available for both of them, in order to set up a communication link.

To address the CCC problem in CR networks, various solutions have been proposed. In particular, several works which fall under the overlay class consider that a spectrum portion is reserved for exchanging control information. This approach has two main drawbacks: if a dedicated channel is selected [3],

the bandwidth available for data traffic transfers reduces; if, instead, a spectrum hole in licensed bands is exploited [4], the CCC has to be “moved” to a different spectrum portion whenever the previous one is occupied by a primary user. Other works, e.g., [2], explore the possibility to set up a network without an a-priori selected CCC, by implementing an in-band signalling scheme on the available channels. Specifically, some CR nodes send (either sequentially or at random) beacon messages on the available channels, while other nodes scan the spectrum. Then, two nodes can establish a direct contact only when one of them receives the beacon transmitted by the other; it follows that meeting a specific device may take a long time.

In this paper, we adopt a different perspective with respect to previous work and consider that the CCC is implemented by using the ultra wide band (UWB) technology¹: each CR node is equipped with an UWB interface, for transmitting/receiving control information, and with one or more radio interfaces (such as IEEE 802.11) for data communication. This solution, which was first proposed in [5], [6], is appealing for the following reasons:

- (1) UWB communication cause negligible interference to narrowband transmissions;
- (2) by using at first a common spreading code, all nodes are able to discover each other over the UWB channel;
- (3) UWB radio interfaces feature very low complexity and power consumption (namely, 1.2 mW, see [7] and references therein);
- (4) although being generally considered a short-range technology, experimental results [5], [8] show that UWB can provide a radio range of about 100 m.

Unlike [5], however, in our work we focus on the implementation of a common control channel for CR users and on the definition of the protocol that lets users discover each other, meet on a channel and establish a communication link when needed. Furthermore, we address the gap in coverage, which typically exists between UWB and medium-long range CR communications technologies, by using the multi-hop transfer paradigm. The protocol was first sketched in our conference paper [6], along with a performance evaluation under a simplistic physical-layer model.

The rest of the paper is organized as follows. We describe

¹We remark that, although the UWB technology is often used for security aspects, in this paper we do not deal with such issues.

our system model in Section II, and highlight how, by exploiting the paradigm of multi-hop communication, UWB can be used for implementing a CCC among CR nodes that want to exchange data traffic through a medium-range technology like 802.11. In Section III, we derive the transmission failure probability on the UWB CCC, while in Section IV we detail the protocol that allows CR nodes to establish a communication link. We show the performance of our solution and compare it to an in-band signalling approach in Section V. Finally, in Section VI we draw some conclusions and discuss future work.

II. SYSTEM MODEL

We consider a communication network composed of N CR nodes. Each node is equipped with an UWB and a medium-long range radio interface, and use them for control and data transmissions, respectively. UWB transmissions are performed by using a spreading code common to all nodes; only after two nodes have got in contact with each other, they can agree on a spreading code to be used for the remaining part of their message exchange on the UWB CCC. As for the medium-long range radio, for concreteness we refer to the IEEE 802.11 technology².

We assume that the UWB CCC is implemented using the Impulse-Radio UWB (IR-UWB) transmission technique. In particular, an M -order pulse position modulation (M -PPM) with time-hopping (TH) is employed. The M -PPM signal transmitted by the generic node n can be written as [10]:

$$s^{(n)}(t) = \sqrt{E_x} \sum_{r=-\infty}^{\infty} x\left(t - rT_f - c_r^{(n)}T_c - \delta u_{[r/N_s]}^{(n)}\right) \quad (1)$$

where $x(t)$ is the reference pulse with unitary energy and duration equal to T_m . Also, E_x is the energy transmitted for each pulse, T_f is the frame duration and $T_c = MT_m$ is the chip duration. The ratio $G = T_f/T_c$, i.e., the number of chip intervals per frame, is called *pulse processing gain*. The hopping sequence of the generic node n , $c_r^{(n)}$, is a sequence of integers in $[0, G-1]$. Finally, $u_b^{(n)}$ is the node binary information sequence, N_s is the bit repetition factor (number of pulses per information bit) and δ is the PPM pulse delay.

In the following, in order to keep the overall signal bandwidth constant, the pulse duration is fixed to $T_m = 2$ ns, for any modulation order M . Also, we set the frame duration $T_f = 258.8$ ns and the symbol duration to $1 \mu s$, again for any modulation order M . For the sake of clarity, Fig. 1 provides an example in the case of the 2-PPM and 4-PPM modulations. Note that, as the modulation order increases, the TH processing gain decreases due to the reduced spectral efficiency of a higher order PPM.

Next, we introduce the physical channel model, which consists of a path loss model and a power delay profile. The model we are considering is derived from [13], where we adopted the parameter values for the CM9 (farm environment). Such a model will be used later in the paper to compute the signal-to-noise-plus-interference ratio (SINR) and the transmission failure probability on the UWB CCC.

²As an example, the use of 802.11 for communications in TV whites spaces has received significant attention, as also shown by recent standardization activities [9].

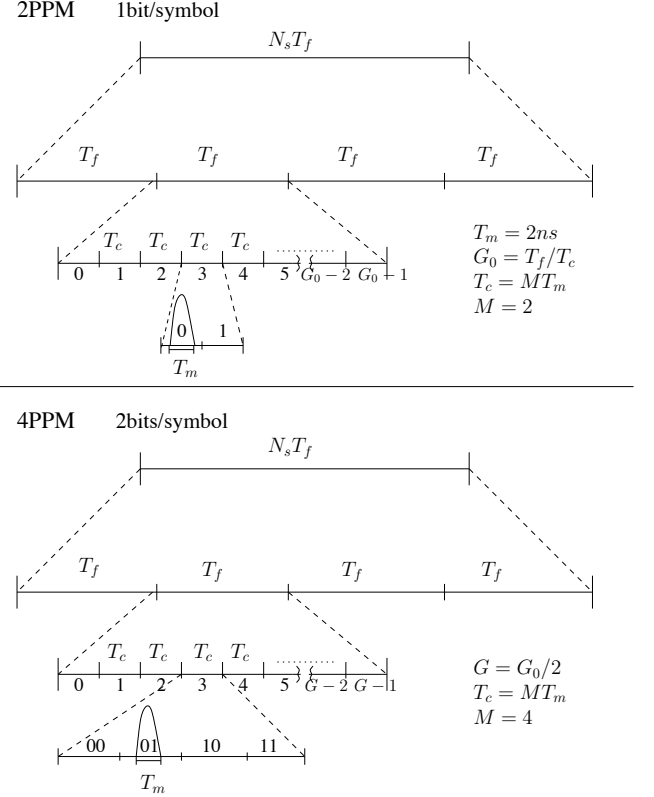


Fig. 1: 2-PPM (top) and 4-PPM (bottom) modulation schemes; the parameter setting used for 2-PPM is taken as a reference.

1) *Path loss model*: Given a generic pair of nodes (i, j) , the path loss between the nodes is modelled as

$$PL_{dB}(d_{ij}) = PL_0 + 10\eta \log_{10} \frac{d_{ij}}{d_0} + S \quad (2)$$

where $PL_0 = 48.96$ dB is the path loss at distance $d_0 = 1$ m, d_{ij} is the Euclidean distance between i and j , $\eta = 1.58$ is the path loss exponent, and the shadowing loss S is a log-normal random variable with zero mean and standard deviation $\sigma = 3.96$ dB.

We assume that the transmitted signal has bandwidth $B = 500$ MHz and the transmitted power spectral density matches the FCC limit for the 3.1 to 10.6 GHz frequency range, which equals -41.3 dBm/MHz [11]. The resulting transmitted power is $P_{T,dBm} = -14.38$ dBm (36.5 μ W), and the received power at j is given by:

$$P_{R,dBm}^{(i,j)} = P_{T,dBm} - PL_{dB}(d_{ij}). \quad (3)$$

2) *Power-delay profile model*: The adopted model is obtained by simplifying the well-known Saleh-Valenzuela (SV) model originally proposed in [12]. According to the SV model, the impulse response of the channel consists of L clusters, each composed of K rays:

$$h(t) = \sum_{l=0}^L \sum_{k=0}^K a_{k,l} e^{j\phi_{k,l}} \delta(t - T_l - \tau_{k,l}) \quad (4)$$

where $a_{k,l}$ is the tap weight of the k -th component in the l -th cluster and $\phi_{k,l}$ is uniformly distributed in $[0, 2\pi)$. T_l is the

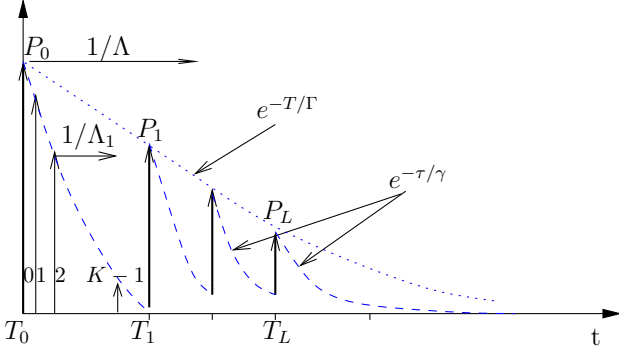


Fig. 2: A representation of the channel impulse response.

l -th cluster delay and $\tau_{k,l}$ is the delay of the k -th ray relative to T_l (with $\tau_{0,l} = 0$).

Also, as done in [12], the number of clusters L is assumed to be a Poisson-distributed random variable with mean equal to 3.31, while the cluster inter-arrival time is assumed to be exponentially distributed with rate 0.0305 ns^{-1} . The ray inter-arrival time is also assumed to be exponentially distributed with rate 0.0225 ns^{-1} . A typical channel impulse response is shown in Fig. 2.

The power of clusters and rays is determined as [12]

$$E\{|a_{k,l}|^2\} \propto \Omega_l \exp(-\tau_{k,l}/\gamma_0) \quad (5)$$

where $\gamma_0 = 0.92 \text{ ns}$ and Ω_l is the integrated energy of the l -th cluster. Ω_l is such that:

$$10 \log(\Omega_l) \propto 10 \log(\exp(-T_l/\Gamma)) + M_{cl} \quad (6)$$

with $\Gamma = 56 \text{ ns}$ and M_{cl} being a zero-mean Gaussian random variable with standard deviation $\sigma_{cl} = 3 \text{ dB}$ [13]. We observe that, within each cluster, the ray energy decay constant γ_0 is less than the pulse duration. Hence, in order to simplify our model, we will consider only one ray per cluster.

III. TRANSMISSION FAILURE PROBABILITY

Following the model introduced above, we characterize the signal propagation over the channel between the generic nodes i and j through the number of clusters $L^{(i,j)}$ and the delay profile $T_0^{(i,j)}, \dots, T_L^{(i,j)}$.

In order to derive the transmission failure probability between i and j , however, we need to refer to a time-discrete power-delay profile and compute the SINR experienced by j when i transmits. To this end, we first define the discretized cluster delay profile as $\tilde{T}_0^{(i,j)}, \dots, \tilde{T}_L^{(i,j)}$ where

$$\tilde{T}_l^{(i,j)} = \left\lfloor \frac{T_l^{(i,j)}}{T_c} \right\rfloor. \quad (7)$$

Here, $T_l^{(i,j)}$'s are random delays generated according to the distribution of the cluster inter-arrival time, truncated to T_f . In other words, the randomly-generated delays that exceed the frame transmission interval T_f are discarded. Hence, the discrete cluster delays are integers in the range $[0, G-1]$.

We can then define the time-discrete power profile as the vector $P_0^{(i,j)}, \dots, P_{G-1}^{(i,j)}$, where

$$P_\theta^{(i,j)} \propto \exp(-gT_c/\Gamma) + 10^{M_{cl}/10}, \quad \theta \in [0, G-1] \quad (8)$$

if there is a value l for which $g = \tilde{T}_l^{(i,j)}$; otherwise, $P_\theta^{(i,j)} = 0$.

We assume that the receiver consists of a single correlator matched to the UWB ray with the highest power, i.e., $P_0^{(i,j)}$. Such an assumption corresponds to a single-finger *rake* receiver locked to the strongest multipath component, like the *selective rake* structure proposed in [14]. The delay of the strongest path is assumed to be perfectly estimated through correlation with the synchronization header. Without loss of generality, we assume that the useful transmission (strongest ray of the useful transmitter) occurs in the first chip interval of each frame, while other transmissions, thanks to the use of different hopping sequences, occur in all chip intervals. As a result, interference occurs when one or more clusters of interfering nodes fall into the first chip interval.

The useful bit energy E_b can therefore be computed as $P_0^{(i,j)} T_f N_s / \log M = P_0^{(i,j)} T_b$.

As for the interfering power, if the useful transmission employs a distinct hopping code, an integer random variable $\theta_{n,f}$, uniformly distributed in $[0, G)$, is generated for each frame and for each interfering node n . Then, the interference energy is computed for each transmitted bit as

$$P_{I,DC} = \sum_{n \in \mathcal{I}_{DC}} \sum_{f=0}^{N_s-1} \tilde{P}_{\theta_{n,f}}^{(n,j)} \quad (9)$$

where \mathcal{I}_{DC} is the set of interfering nodes that employ hopping sequences distinct from node i (the node whose signal j wants to receive). The above expression is also used to compute the interference when both the useful and the interfering signals use the common code but they start at different time instants.

If, instead, the useful transmission employs a common hopping code, the interference from all nodes transmitting with such a code must be taken into account:

$$P_{I,CC} = \sum_{n \in \mathcal{I}_{CC}} \sum_{f=0}^{N_s-1} \tilde{P}_{\theta_n}^{(n,j)} \quad (10)$$

where \mathcal{I}_{CC} is the set of interfering transmitters that use the common hopping sequence, and θ_n is an integer random variable uniformly distributed in $[0, G-1]$ and *constant* for the whole packet transmission.

The SINR for every bit transmission from i to j can therefore be computed as

$$\text{SINR}^{(i,j)} = \frac{P_0^{(i,j)}}{P_{I,DC} + P_{I,CC} + N_0 B} \quad (11)$$

where $P_0^{(i,j)}$ is given by the expression in (3). The SINR computed in this way takes into account the reduced power of the useful signal resulting from the adoption of a single-correlator receiver, and, by accounting for the power-delay profiles of interfering nodes, it provides an accurate estimate of the interference power.

By using the above expression for the SINR, we can then obtain the expression for the bit error probability over the link between i and j . In particular, in the case of a 2-PPM, the bit error probability is given by

$$P_b^{(i,j)}(e) = \frac{1}{2} \text{erfc} \sqrt{\frac{\text{SINR}^{(i,j)}}{2}} \quad (12)$$

while, for $M > 2$, we use the union bound approximation and write:

$$P_b(e)^{(i,j)} \leq \frac{M}{4} \operatorname{erfc} \sqrt{\frac{\log_2 M}{2} \frac{E_b}{N_0}}. \quad (13)$$

The error rate of the radio channel is then improved by employing a Forward Error Correcting (FEC) technique. Due to their low complexity, good performance and widespread usage, Bose-Chaudhuri-Hocquenghem (BCH) codes [15, Ch.10] are adopted. The code word length, information word length and error correction capability are chosen to match the packet lengths of the exchanged messages. Moreover, in order to enable the receiver to detect the message integrity, after channel decoding, an 8-bit cyclic-redundancy-check (CRC) code is added. If, during a message transmission, the total number of bits in error within a code word exceeds the error correction capability of the code, then the message transmission fails. This model will be used in our simulations to derive the performance results.

IV. THE UWB COMMON CONTROL CHANNEL IMPLEMENTATION

Given the network system described above, we assume that, on a regular basis, all CR nodes transmit and receive through their UWB interface by using a common spreading code. Only after two nodes have got in contact with each other, they can continue their message exchange on the UWB CCC by using a distinct spreading code, which is randomly selected by the exchange initiator out of a set of available codes.

Below, we detail the message exchange on the UWB channel that allows CR nodes to build their knowledge on the network topology, as well as to meet and establish a communication link on a data channel. Note that, as UWB is a short-range communication range, in order to get in contact with a candidate 802.11 data receiver, a source may need to use relay nodes while operating on the UWB CCC. We therefore identify multi-hop communication as a means to overcome the gap in coverage between UWB and medium-long range technologies, and we define the communication protocol for link set up in both the cases of single- and multi-hop UWB communication.

A. Discovering the network topology

All network nodes periodically broadcast a Hello message over the UWB CCC, using the common spreading code. A Hello includes the sender's identifier (ID), as well as the ID of the x -hop UWB neighbors the sender is aware of, with $x = 1, \dots, h - 1$. Specifically, given node i , it tags node j as its one-hop neighbor upon successfully receiving a Hello from j , and it tags all of j 's x -hop neighbors (from which i has not received a Hello) as its $(x + 1)$ -hop neighbors. By doing so, even in a dynamic scenario where nodes may join or move out of the network, every CR device knows the nodes with which it can directly communicate over the UWB channel, or that can be reached in up to h hops. An example is depicted in Fig. 3, where the UWB maximum radio range is half the one provided by the 802.11 interface, i.e., $h = 2$.

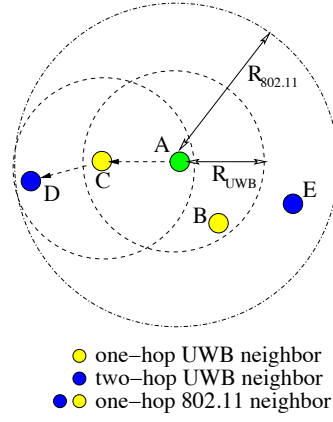


Fig. 3: UWB and 802.11 neighbors: an example. A has B and C as one-hop UWB neighbors, D and E as two-hop UWB neighbors, and B , C , D , and E as one-hop 802.11 neighbors.

TABLE I: CCC routing table at node A

Destination ID	Next-hop ID	Distance (#hop)
B	B	1
C	C	1
D	C	2
E	B	2

Now, let us consider a newly arrived CR device wishing to communicate with other nodes. By using its UWB interface, the newly arrived device listens to the common code channel and waits for Hello messages from nearby nodes. If it does not hear any Hello message within a given time interval, it broadcasts on the UWB CCC a Join Request Message (JRM), which is transmitted using the common spreading code. The JRM includes the IDs of the sender and of the selected spreading code. Upon receiving the JRM message, a one-hop neighbor replies using the selected code, with a unicast packet called Join Answer Message (JAM). The JAM is transmitted after a random time since the JRM reception, so as to avoid collisions among different replies; it carries the list of nodes that are the x -hop UWB neighbors of the sender, with $x = 1, \dots, h - 1$.

Through the above message exchange (i.e., Hello, JRM, and JAM messages), a CR node can acquire or update the structure of the network topology, up to a distance of h UWB hops. It can therefore build/maintain a *CCC routing table* where it records the list of nodes it can reach through one- or multi-hop UWB transmissions. More specifically, each entry in the CCC routing table of a CR device will include the ID of the destination node, the ID of the next-hop node that allows the device to reach that destination with the minimum number of hops, and the distance in number of hops from the destination. An example, which refers to the topology in Fig. 3, is reported in Tab. I.

B. Establishing a data link

CR devices can use CCC routing tables to set up 802.11-based links with other nodes.

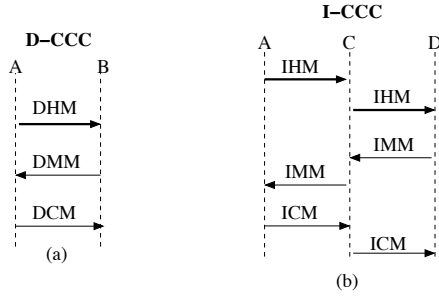


Fig. 4: Message exchange between initiator and destination nodes. Messages transmitted using the common and the selected spreading codes are denoted by the thick and the thin line, respectively. In (a), A and B are one-hop UWB neighbors, while in (b) A , C and D act as initiator, relay and destination nodes, respectively.

As an example, let us first consider that node A in Fig. 3 wishes to establish a data communication with node B which, according to A 's CCC routing table, is one of its one-hop UWB neighbors. In this case, A will use the common spreading code to contact B . In particular, A will send a Direct Handshake Message (DHM) including the set of channels that A senses as available, ordered according to their quality level, and the preferred channel to be selected for communication through the 802.11 interface. Also, A will include in the DHM its own ID, the destination ID, and the ID of the spreading code that A has randomly selected among the available ones. This code will be used for exchanging the following control messages so as to reduce the channel interference level.

By using the selected code, B replies with a Direct Matching Message (DMM) that carries several important information. Firstly, it indicates whether A 's selection has been accepted, or if another channel (among the ones listed by A) is proposed; secondly, it includes a backup channel that B identifies based on the channel list provided by A and its own list; thirdly, it makes the information exchange about the available channels list symmetric, by including the list of channels that B senses as available, ordered according to their quality level. Finally, A sends a Direct Confirmation Message (DCM) to B (again using the chosen spreading code); afterwards the 802.11-based communication on the selected channel can start. Fig. 4(a) reports the message exchange described above.

We point out that, during the above message exchange, if a node does not receive the reply message associated to its transmission within a given timeout, it waits for a random time (backoff time) and then it sends the message again. As a maximum number of attempts is reached, the message is discarded. When instead the message exchange is successful and the data communication starts but, at a certain point in time, a primary user shows up on the selected data channel, A and B can both switch onto the (previously agreed) backup channel and continue their data communication there.

Now, let us consider that A wants to communicate with node D , which is a two-hop UWB neighbor. Then, multi-hop communication on the UWB CCC has to be employed. According to its CCC routing table, A sends an Indirect

Handshake Message (IHM) to the next-hop node C , by using the common spreading code. The IHM includes the IDs of the sender, of the next-hop node and of the final destination, as well as the list of channels sensed as idle by A with their associated quality level. As before, the IHM also carries the ID of the randomly selected spreading code to be used for transmitting the following messages. Once the relay node, C , receives the IHM, it forwards the message toward the final destination (still using the common code). By using the selected code, the destination D will reply with an Indirect Matching Message (IMM) that contains the same information as a DMM, but it is relayed back toward the handshake initiator. A then transmits an Indirect Confirmation Message (ICM) to the destination. Afterwards the data communication between A and D can start on the selected channel, through the medium-long range radio.

Fig. 4(b) summarizes the message exchange between initiator, relay and destination nodes. Note that, in this case, implicit acknowledgments ("passive ACKs") are used at the initiator node (A in our example) by monitoring transmissions by the relay node (i.e., C). If the initiator hears the relay retransmitting the message within a timeout, the transmission is considered to be successful; otherwise it is considered to be a failure. As for the relay node, it considers its own transmission to be a failure if it does not receive the reply message associated to the transmission within a timeout. In the case of failure, both initiator and relay nodes carry out a backoff procedure as described for the single-hop case.

V. PERFORMANCE EVALUATION

Here, we first detail the simulation scenario, then we show the performance of our solution when CR nodes wish to establish a communication link for data traffic. The results have been derived through extensive simulation runs and taking into account all the details of the UWB system model previously described.

A. Reference scenario

We consider N static nodes, which are randomly deployed according to a uniform distribution in a square region of side equal to 250 m. As a node wishes to start a traffic flow, it accesses the UWB channel using the Aloha scheme. The length of the spreading codes is equal to 176 chips, while the UWB data rate is 966 kb/s [16], and we consider M -PPM modulations with $M = 2, 4, 8, 16$.

The timeout used at the one hop initiator and relay nodes is set to 2.5 ms, while the timeout used at the multihop initiator is set to 25 ms; in the case of failure a message can be retransmitted up to four times, using a backoff time that is randomly selected in the range $[0, 2.5 \text{ ms}]$ and $[0, 25 \text{ ms}]$ for direct and multi-hop messages, respectively. Moreover, when a node receives a passive acknowledgment from its next-hop node, i.e., it overhears the relay forwarding its message, it sets its timeout timer to 1 s.

As for IEEE 802.11-based communication, we assume that 12 channels are available for data traffic and they are sensed with the same quality level by all CR nodes. The physical layer

synchronization header of the packets exchanged on the UWB channel is set to 8 bytes [16]; their length, however, depends on the type of control information they carry. More specifically, we set the size of the ID field equal to 6 bytes, the size of the channel list field to 6 bytes (being the number of data channels equal to 12 and the channel ID encoded onto 4 bits) and the CRC to 1 byte, while the ID of the selected spreading code is encoded onto 4 bits. Thus, the size of the largest message (i.e., the DHM) at the input of the BCH encoder is equal to 20 bytes. Finally, we consider a (255,239,2) BCH code, shortened to match the message length; such code adds 16 redundancy bits to each message and its error correction capability is equal to 2 bits.

B. Results

We consider the network scenario described above and derive the system performance when a communication link has to be established between CR nodes, through single-hop or multi-hop transmissions. For the latter case, in our scenario we observed that the maximum number of hops between source and destination is limited to $h = 2$ hops, when the receiver sensitivity equals³ -95 dBm.

Fig. 5 presents the success probability of single messages transmitted on the UWB CCC (top plot), and of the complete message handshake needed to set up a communication link (bottom plot). Results are shown in both the cases of one-hop and multi-hop transmissions, in the plot referred to as D-CCC and I-CCC, respectively; also, we set the per-node flow rate $\lambda = 0.5$ and vary the number of nodes N as well as the modulation order (namely, $M = 2, 4, 8, 16$). We observe that better performance is obtained for high order PPMs. Furthermore, the success probability of complete handshakes carried out through direct transmissions is always higher than for single-message transmissions. Indeed, the latter is computed as the ratio of the number of successful messages to the total number of messages sent over the channel (transmissions and retransmissions). Thus, the probability to complete a handshake is higher than the message success probability, since failed messages can be retransmitted and, if eventually successful, they lead to a successful handshake. On the contrary, the success probability for complete handshakes, carried out through multi-hop transmissions and for a high number of nodes, is always lower than for single-message transmissions. Indeed, the message success probability is still computed over a single hop, while a handshake now is successful only if all message transmissions are eventually successful over two-hops, which is has a lower chance to occur.

Finally, as expected, the number of nodes N has an impact on the system performance since the higher the number of nodes, the higher the interference level experienced by a receiver. A similar observation holds when we let the per-node flow rate λ increase. However, we stress that very good results are achieved, even for values of λ and N as large as 0.5 and 40, respectively, for both the single- and multi-hop CCC case.

³This is a typical value chosen in the literature.

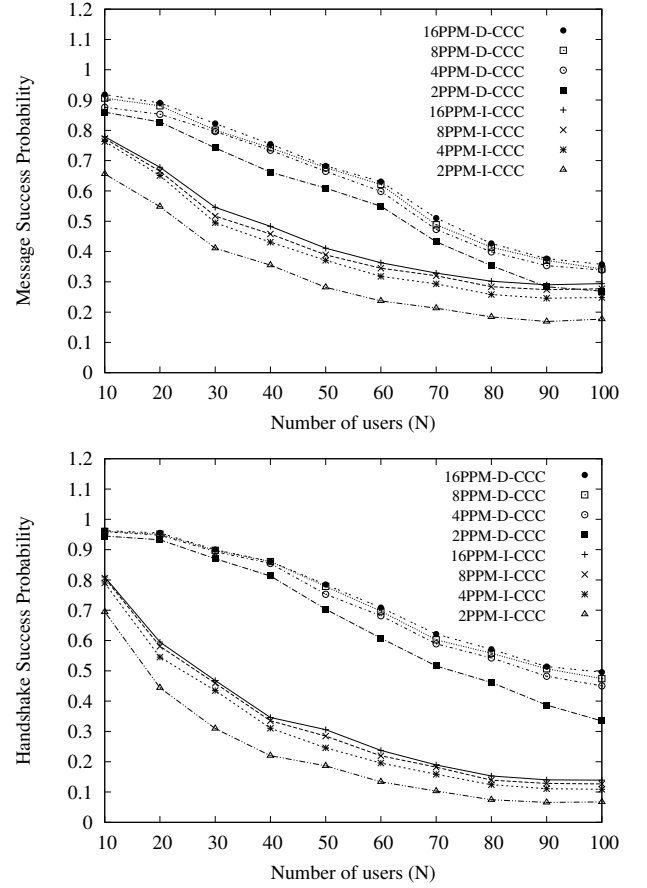


Fig. 5: Success probability for single messages (top) and complete message handshakes (bottom), as N varies and $\lambda = 0.5$ and. The labels D-CCC and I-CCC refer to the single- and multi-hop CCC, respectively.

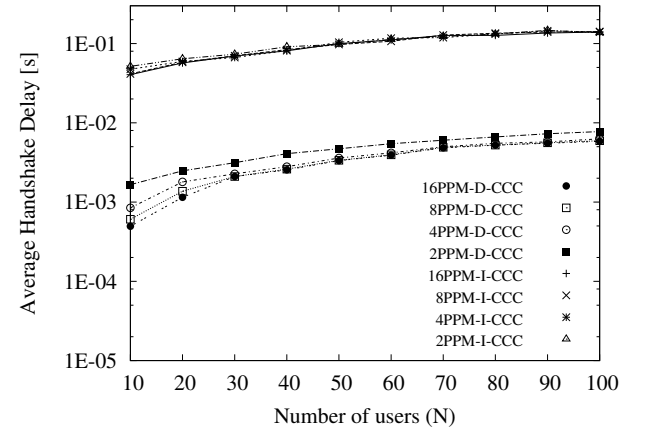


Fig. 6: Average handshake delay for the single- and multi-hop CCC, when N varies and $\lambda = 0.5$. The results obtained with different modulations are compared.

Fig. 6 represents the average handshake delay over the single-hop CCC (D-CCC) and multi-hop CCC (I-CCC), for $\lambda = 0.5$ and as N varies. We note that, for D-CCC, the average duration of a successful message handshake is in the order of milliseconds, for any value of N we considered, and the 16-PPM provides an average delay that is about half the value

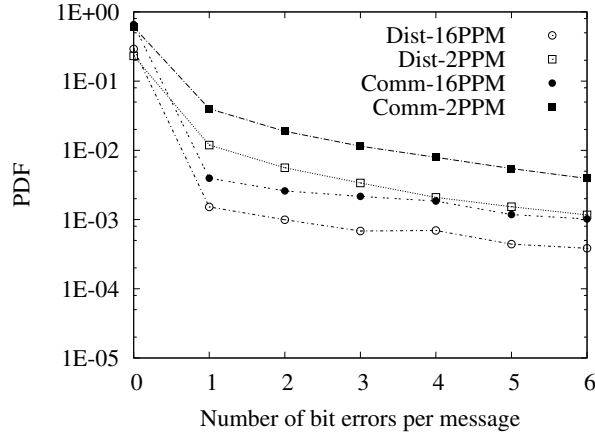


Fig. 7: Probability density function of the number of bit errors per message, in the cases of common and distinct codes and for $N = 50$ and $\lambda = 0.5$. The performance obtained with 2-PPM and 16-PPM are compared.

yielded by the 2-PPM. This is due to the fact that, when the 16-PPM is used, transmission durations are shorter and, thus, the interference level is lower than in the 2-PPM case (as also confirmed by the results in Fig. 5). Looking at the I-CCC average delay, we also observe that the duration of a successful message handshake is in the order of tens of milliseconds, for any value of N , and the 16-PPM and 2-PPM provide almost the same average value.

Looking at Figs. 5 and 6, we note that the 16-PPM and 2-PPM give the best and worst performance, respectively. In the following, we will then focus on these modulations and omit the results obtained for intermediate values of M .

Fig. 7 shows the probability density function of the number of bit errors per message at the input of the BCH decoder. We compare the 2-PPM and 16-PPM in both cases, when the sender is using common and distinct codes. As expected, the probability of bit errors in case of common codes is higher than in the case of distinct codes. Fig. 8 also shows the probability density function of having at most 2 or 4 bit errors at the input of the encoder. By looking at the results, we can observe that the BCH code we selected fits well our goals, and that a BCH code with higher error correction capability would not provide any significant improvement.

Next, one may wonder what distance can be covered by direct transmissions over the single-hop UWB CCC, with an acceptable handshake success probability. To answer this question, in Fig. 9 we show the success probability of a message handshake over the D-CCC, as the distance between source and destination nodes varies. We set $N = 10, 50, 100$ and use the 2-PPM modulation. Interestingly, for $N = 10$, UWB communication allows nodes that are even farther than 130 m away to successfully get in contact with each other, with high probability. As the number of network nodes grows, the handshake success probability decreases, but still we achieve good performance for values of N as large as 100 and a distance between source and destination of about 50 m. Such results are confirmed by the plot in Fig. 10, which shows the probability density function of the SINR experienced in the

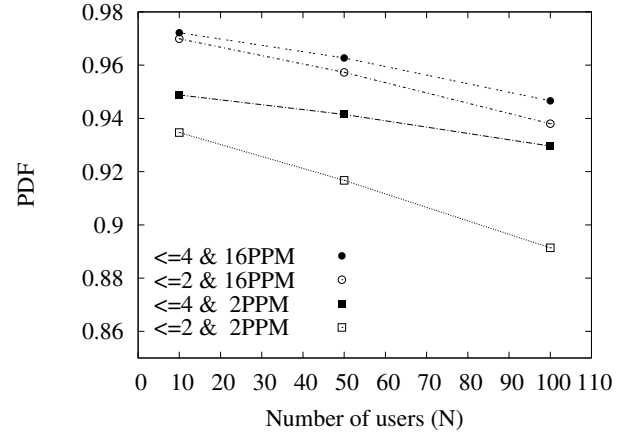


Fig. 8: Probability density function of having 2 or 4 bit errors at most, at the input of the encoder. The performance obtained with 2-PPM and 16-PPM are compared for different values of N and $\lambda = 0.5$.

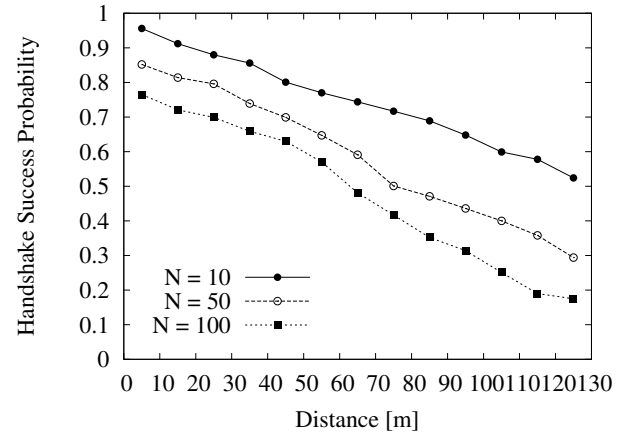


Fig. 9: Handshake success probability over the UWB single-hop CCC as a function of the distance between source and destination, for different values of N , $\lambda = 0.5$ and when the 2-PPM modulation is used.

case of the 2-PPM, $N = 100$ and $\lambda = 0.5$.

Figs. 11 and 12 present the probability density function of having $1, \dots, N - 1$ interferers in the case of 2-PPM and 16-PPM, respectively (curves labeled by “Total”). We set $N = 100$ and $\lambda = 0.5$. The same plots depict the conditioned probability that, given i interferers ($i = 1, \dots, N - 1$), they are at 1, 2, or more than 2 hops away. We observe that the total number of interferers in the case of 2-PPM is higher than for 16-PPM. Indeed, as noticed earlier, the 16-PPM implies shorter transmission durations, hence that simultaneous transmissions are less likely to take place.

Finally, Fig. 13 shows the comparison between the performance of the UWB-CCC and the in-band signalling schemes. The latter is an enhanced, distributed version of the so-called EX mechanism, which has been proposed in [2]. The handshake success probability and average delay are presented as the number of CR users varies. Note that, for the in-band signalling solution, the handshake corresponds to the beacon-acknowledgment message exchange between the source user

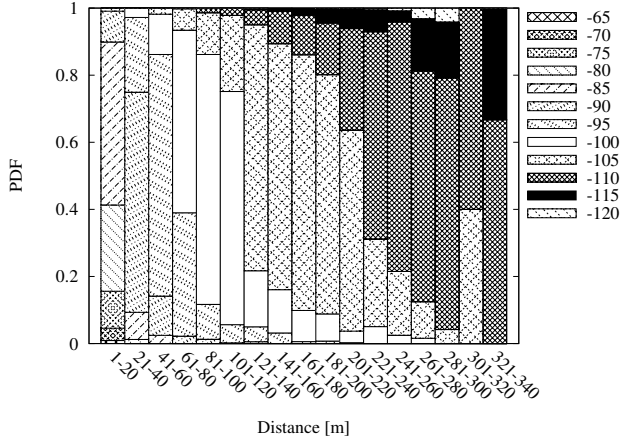


Fig. 10: Probability density function of the experienced SINR, for $N = 100$ and $\lambda = 0.5$, and when the 2-PPM modulation is used.

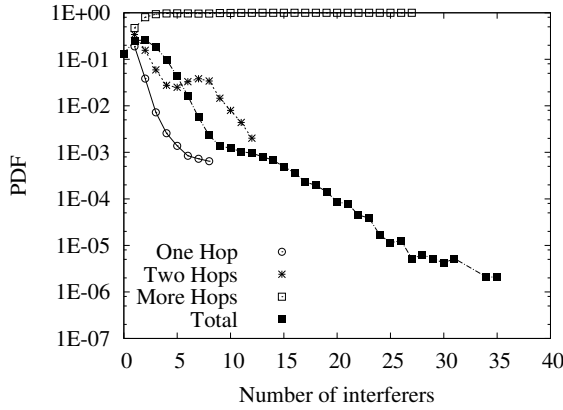


Fig. 11: Probability density function of having $1, \dots, N - 1$ interferers (curve labeled by “Total”) when the 2-PPM is used and for $N = 100$ and $\lambda = 0.5$. The conditioned probabilities that, given i interferers ($i = 1, \dots, N - 1$), they are at 1, 2, or more than 2 hops away are also shown.

and the intended destination. Also, the results for the UWB-CCC case have been derived by assuming a 2-PPM, which, as highlighted earlier in this section, represents the worst case relatively to other modulation orders.

From the top plot in Fig. 13, it is clear that the UWB CCC implies a significantly higher success probability, especially when the number of users increases. Looking at the bottom plot, we can also see that the UWB CCC outperforms the in-band signalling solution in terms of average handshake delay. Specifically, it provides a latency reduction in making contact between source and destination of about one order of magnitude.

VI. CONCLUSIONS

We addressed the problem of establishing a common control channel in cognitive radio networks, by exploiting the UWB technology. We identified multi-hop communication as a means to overcome the gap in coverage that typically exists between UWB and medium-long range technologies,

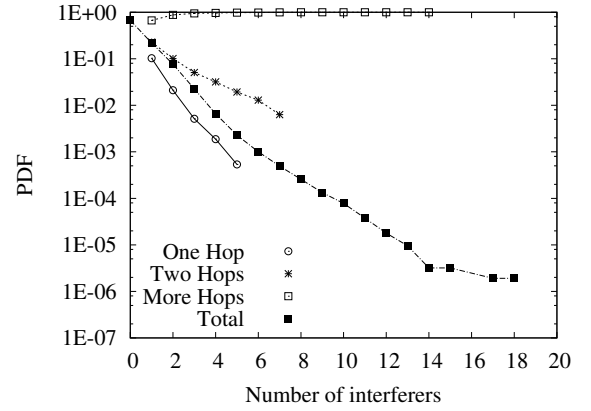


Fig. 12: Probability density function of having $1, \dots, N - 1$ interferers (curve labeled by “Total”) when the 16-PPM is used and for $N = 100$ and $\lambda = 0.5$. The conditioned probabilities that, given i interferers ($i = 1, \dots, N - 1$), they are at 1, 2, or more than 2 hops away are also shown.

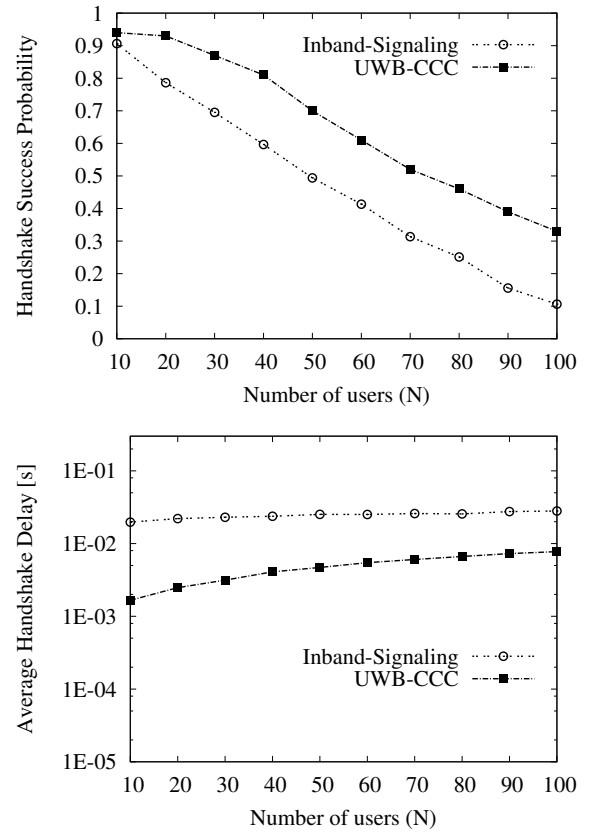


Fig. 13: Handshake success probability (top) and average handshake delay (bottom), vs. number of users. The UWB-CCC and the in-band signalling solutions are compared.

and we defined the communication protocol needed to let cognitive radio nodes discover each other and exchange control information for link set up.

Our simulation results, obtained under an accurate channel model, highlighted that: (i) 16-PPM outperforms lower-order modulations, (ii) the use of both a single- and a multi-hop common control channel allows cognitive radio nodes to meet

and agree on a data communication channel with very good success probability and small latency, (iii) an UWB common control channel allows nodes, which are even 100 m far away from each other, to successfully get in contact with each other with high probability, and (iv) the UWB-based approach can significantly outperform an in-band signalling solution, in terms of both probability of success and latency in establishing a contact. Future work will further evaluate the performance of the proposed solution in presence of mobile nodes and of different channel access schemes.

REFERENCES

- [1] B. F. Lo, "A survey of common control channel design in cognitive radio networks," *Physical Communications*, Jan. 2011.
- [2] Y. R. Kondareddy, P. Agrawal, K. Sivalingam, "Cognitive radio network setup without a common control channel," *IEEE MILCOM*, Nov. 2008.
- [3] I. Akyildiz, W.-Y. Lee, M. C. Vuran, M. Shantidev, "NeXt generation/dynamic spectrum access/cognitive radio wireless networks: A survey," *Computer Networks*, vol. 50, no. 13, Sep. 2006, pp. 2127–2159.
- [4] J. Zhao, H. Zheng, G.-H. Yang, "Distributed coordination in dynamic spectrum allocation networks," *IEEE DySPAN*, Nov. 2005.
- [5] M. E. Sahin, H. Arslan, "System design for cognitive radio communications," *Int. Conf. on Cognitive Radio Oriented Wireless Networks and Commun. (CrownCom 2006)*, Mykonos Island, Greece, June 2006.
- [6] A. Masri, C.-F. Chiasserini, A. Perotti, "Control information exchange through UWB in cognitive radio networks," *IEEE International Symposium on Wireless Pervasive Computing, (ISWPC)*, Modena, Italy, July 2010.
- [7] A. Gerosa, M. Dalla Costa, A. Bevilacqua, D. Vogrig, A. Neviani, "An energy-detector for non-coherent impulse-radio UWB receivers," *IEEE Transactions on Circuits and Systems - I*, vol. 56, no. 5, May 2009.
- [8] J. Nascimento, H. Nikookar, "On the range-data rate performance of outdoor UWB communication," *2nd Intl. Conf. on Wireless Broadband and UWB Communications*, 2004.
- [9] IEEE 802.11 activities. http://www.ieee802.org/11/QuickGuide_IEEE_802_WG_and_Activities.htm
- [10] G. Durisi, S. Benedetto, "Performance evaluation of TH-UWB systems in the presence of multiuser interference," *IEEE Communication Letters*, vol. 7, no. 5, pp. 224–226, May 2003.
- [11] Federal Communications Commission, "Revision of part 15 of the commission's rules regarding Ultra-Wideband transmission systems," ET-Docket 98-153, Washington, D.C., Apr. 2002.
- [12] A. A. M. Saleh, R. A. Valenzuela, "A statistical model for indoor multipath propagation," *IEEE Journal on Selected Areas in Communications*, vol. 5, no. 2, pp. 128–137, Feb. 1987.
- [13] A. F. Molisch, D. Cassioli, C.-C. Chong, S. Emami, A. Fort, B. Kannan, J. Karedal, J. Kunisch, H. G. Schantz, K. Siwiak, M. Z. Win, "A comprehensive standardized model for ultrawideband propagation channels," *IEEE Transactions on Antennas and Propagation*, vol. 54, no. 11, Nov. 2006.
- [14] D. Cassioli, M. Z. Win, F. Vatalaro, A. F. Molisch, "Low complexity rake receivers in ultra-wideband channels," *IEEE Transactions on Wireless Communications*, vol. 6, no. 4, pp. 1265–1275, Apr. 2007.
- [15] S. Benedetto, E. Biglieri, *Principles of digital transmission with wireless applications*, New York: Plenum/Kluwer Publishers, 1999.
- [16] M. G. Di Benedetto, L. Nardis, G. Giancola, "The Aloha access (UWB)² protocol revisited for IEEE 802.15.4a," University of Rome La Sapienza, Italy, *ST Journal of Research*, vol. 4, no. 1, pp. 131, May 2007.